



**AFRL-RX-WP-JA-2017-0210**

**FERROELECTRIC BaTiO<sub>3</sub> AND LiNbO<sub>3</sub> NANOPARTICLES  
DISPERSED IN FERROELECTRIC LIQUID CRYSTAL  
MIXTURES: ELECTROOPTIC AND DIELECTRIC  
(POSTPRINT)**

**R.K. Shukla and W. Haase**

**Technische Universität Darmstadt**

**D.R. Evans**

**AFRL/RX**

**17 September 2016  
Interim Report**

**Distribution Statement A.  
Approved for public release: distribution unlimited.**

**© 2016 TAYLOR & FRANCIS GROUP, LLC**

**(STINFO COPY)**

**AIR FORCE RESEARCH LABORATORY  
MATERIALS AND MANUFACTURING DIRECTORATE  
WRIGHT-PATTERSON AIR FORCE BASE, OH 45433-7750  
AIR FORCE MATERIEL COMMAND  
UNITED STATES AIR FORCE**

# Ferroelectric BaTiO<sub>3</sub> and LiNbO<sub>3</sub> nanoparticles dispersed in ferroelectric liquid crystal mixtures: Electrooptic and dielectric parameters influenced by properties of the host, the dopant and the measuring cell

R. K. Shukla<sup>a,c</sup>, D. R. Evans<sup>b</sup>, and W. Haase<sup>a</sup>

<sup>a</sup>Eduard-Zintl-Institut für Anorganische und Physikalische Chemie, Technische Universität Darmstadt, Germany; <sup>b</sup>Air Force Research Laboratory, Materials and Manufacturing Directorate, Wright-Patterson Air Force Base, Ohio, USA; <sup>c</sup>Department of Physics, DIT University, Dehradun, Uttarakhand, India

## ABSTRACT

Harvested ferroelectric nanoparticles of BaTiO<sub>3</sub> and LiNbO<sub>3</sub> were dispersed in Ferroelectric Liquid Crystals (FLCs) with very high spontaneous polarization (*P*<sub>s</sub>). The electrooptic and dielectric parameters were documented. The dipoles of ferroelectric nanoparticles and those of FLCs are partially cancelled in an antiparallel manner. The role of cell parameters like thickness of the Nylon 6 polymer layer and the change in preparation of the polymer layer due to different mechanical rubbing cycles has been described for one high-*P*<sub>s</sub> FLC and for high-*P*<sub>s</sub> FLC/BaTiO<sub>3</sub> nanocolloids. Cell properties depend strongly on anchoring forces which might interact with dipoles both from ferroelectric nanoparticles and high-*P*<sub>s</sub> FLCs.

## ARTICLE HISTORY

Accepted 29 June 2016

## KEYWORDS

Ferroelectric liquid crystals; solid state ferroelectrics; FLC-nanocomposites; surface phenomena

## Introduction

Nematic Liquid Crystals are unique soft materials, widely used in the modern technological world in TVs, displays, smartphones etc. Still there is a need for improving parameters of Nematic Liquid Crystals allowing for rapidly changing moving pictures during the time frame below about 5-10 *ms*. Ferroelectric Liquid Crystals (FLCs) could fill this gap bearing some advantages over Nematic Liquid Crystals, mainly a fast switching time in the microsecond range, better optical contrast, and low threshold voltage. FLCs are layered Liquid Crystals, tilted and containing a chiral group within the molecule [1,2]. Numerous suggestions for applying FLCs in fast moving devices have been described, but even for FLCs there is a need for improving relevant properties. For instance the stability against mechanical attacks is a critical point. In this context improving material aspects is important, but even the optimization of cell parameters must be taken into consideration. Recently, Lapanik et al. [3] presented a way to overcome the problem of mechanical instability of FLCs just by selecting proper compositions. On the other hand for nematic chiral LCs switching processes could be improved leading to switching times of chiral nematics down to the level of

**CONTACT** W. Haase  [haase@chemie.tu-darmstadt.de](mailto:haase@chemie.tu-darmstadt.de)

Color versions of one or more of the figures in the article can be found online at [www.tandfonline.com/gfer](http://www.tandfonline.com/gfer).

© 2016 Taylor & Francis Group, LLC

microseconds [4]. There is space for improving the FLC properties but even for the case of (chiral) Nematics.

Recently very strong activities have been started to work with and understand the function of nanoparticles dispersed in both Nematic and Ferroelectric Liquid Crystals. Fascinating results were documented in [5]. Nano dopants used are from different functionalities such as Single- or Multiwalled Carbon Nanotubes, Graphene, CdSe-dots, and many more. The aim of this investigation is to study the influence of nanoparticles dispersed in liquid crystals on physical properties, and even search for improving relevant parameters, for instance the switching time.

Among other topics we are interested in ferroelectric nanoparticles like BaTiO<sub>3</sub> [6] and LiNbO<sub>3</sub> [7] dispersed in Ferroelectric Liquid Crystals. BaTiO<sub>3</sub> in the tetragonal bulk phase showed a polarization  $26 \mu\text{C}/\text{cm}^2$  whereas LiNbO<sub>3</sub>  $71 \mu\text{C}/\text{cm}^2$ . After the milling of such solid state ferroelectric materials, the strongest dipoles were selected via harvesting under a large electric DC field gradient [8,9] leading to applicable nanoparticles for preparation of FLC nanocolloids. Due to the incorporation of ferroelectric nanoparticles in different FLC mixtures the electro-optical parameters were remarkably changed.

In detail BaTiO<sub>3</sub> harvested nanoparticles of three different sizes and of two different concentrations were dispersed in three different FLC mixtures showing different values of spontaneous polarization ( $P_s$ ) [6]. With help of electrooptic and dielectric methods the FLC/BaTiO<sub>3</sub> nanocolloids were investigated. Similar results were obtained in [10] and [11] for FLC/BaTiO<sub>3</sub> nanocomposites studied on non- harvested materials.

LiNbO<sub>3</sub> was investigated only for nanoparticles of  $25 \text{ nm}$  averaged size but different concentration in a different FLC mixture resulting in a  $P_s$  of about  $65 \text{ nC}/\text{cm}^2$  at room temperature for a cell of thickness  $1.5 \mu\text{m}$  [7].

Cell properties dependent on the electrooptic parameters of FLCs were selectively presented in the literature. An updated overview has been given very recently by Prakash et al. [12] on the dependence of electrooptic and dielectric properties on the cell thickness. In their work on Surface Stabilized cells with ITO electrodes and polyimide rubbed alignment layers, the electrooptic and dielectric parameters were described for different cell thicknesses. Shashidhar et al. [13] used a FLC with high  $P_s$  ( $\sim 250 \text{ nC}/\text{cm}^2$ ) in a cell, one glass plate patterned with a gold electrode and the other decorated with an ITO electrode and SiO alignment layer: they described no change of  $P_s$  by changing the cell thickness. A strong influence on the electrooptic properties is due to the anchoring energy which has been described as inversely proportional to the switching time [14].

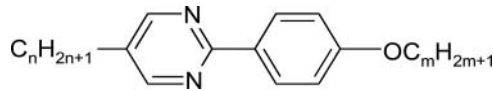
The aim of this contribution is the following: in the first part we wanted to test the electrooptic and dielectric parameters for LiNbO<sub>3</sub> dispersed in a FLC mixture with much higher  $P_s$  ( $\sim 200 \text{ nC}/\text{cm}^2$ ) than used in [7], for a  $2 \mu\text{m}$  thick cell. Next we studied how cell properties influence the electrooptic and dielectric parameters of undoped FLC and doped FLC. As one example, we used different repetitions of rubbing on the polymer layer Nylon 6, this was for BaTiO<sub>3</sub> dispersed in FLC mixture with the acronym *LNSM6* [6]. Finally, we explored how the thickness of Nylon 6 polymer layer influences the electrooptic and dielectric parameters of undoped FLC.

## Experimental

Harvested ferroelectric nanoparticles of LiNbO<sub>3</sub> and BaTiO<sub>3</sub> used in the present study were prepared via a milling technique [8,15]. The detailed procedure of nano particle preparation,

their size estimation, and other basic characterizations are reported elsewhere [6,7]. The average sizes of  $\text{LiNbO}_3$  and  $\text{BaTiO}_3$  nanoparticles used in this study were  $\approx 25 \text{ nm}$  and  $\approx 26 \text{ nm}$  respectively. Harvested nanoparticles of  $\text{LiNbO}_3$  and  $\text{BaTiO}_3$  were capped with 1 wt. % oleic acid to prevent aggregation and reduce the inter-particle interactions [16].

Two distinct ferroelectric liquid crystalline mixtures exhibiting different spontaneous polarizations were selected for this study. The first FLC is with the acronym *LF4*. *LF4* comprised of phenyl pyrimidines compound. The components of the FLCs are shown below



with weight concentrations for  $m = 8, n = 10$  of 43.3%,  $m = 9, n = 8$  of 33.3% and  $m = 8, n = 8$  of 23.4%. The *LF4* mixture exhibited 75:25 wt. % ratios of mesogenic compound and chiral component respectively. Terphenyl is used as a chiral dopant in the prepared FLC mixture, with two chiral  $\text{C}_5\text{H}_{11}\text{CH}^*(\text{CH}_3)\text{-OCO}$  groups in the *p, p'* positions, the chemical structure of chiral dopant is specified in [6,7]. In comparison the same ratio of 2-(4'-alkoxy-phenyl)-4-alkyl-pyrimidines were used for the FLC described in [7], but the ratio of 2-(4'-alkoxy-phenyl)-4-alkyl-pyrimidines and same chiral terphenyl compound compared to [7] was only 90:10 leading to much lower values of  $P_s$ . The chemical composition, structure and acronym used for the second FLC (*LNSM6*) have been previously reported in [6]. For *LNSM6* the ratio of mesogenic compound and chiral component was 79:21 wt. %. To do this work we used in both cases FLC mixtures with higher amount of chiral dopant leading to higher  $P_s$  compared to [6,7].

The phase sequence of ferroelectric mixture *LF4* is (heating cycle)  $25.0^\circ\text{C} - \text{SmC}^* - 65.4^\circ\text{C} - \text{SmA}^* - 69.8^\circ\text{C} - \text{Iso}$  (onset of the  $\text{SmC}^*$  phase may be at  $< 25.0^\circ\text{C}$ ) [7]. The phase sequence for *LNSM6* is  $\text{gl} (10.8^\circ\text{C}) \text{SmC}^* (79.1^\circ\text{C}) \text{SmA}^* (82.1^\circ\text{C}) \text{Iso}$  [6].

In order to prepare nanocolloids, harvested  $\text{LiNbO}_3$  with oleic acid capped nanoparticles were dispersed in heptane. The mixtures were sonicated until they became homogenous (visually examined). Further, 0.01 and 0.1wt%  $\text{LiNbO}_3$  nanoparticles were dispersed in the *LF4* mixture. The colloidal mixtures were heated until full evaporation of the heptane.

A similar procedure was followed to obtain the *LNSM6*/ $\text{BaTiO}_3$  nanocolloids by using chloroform as a dispersion medium. The percentage of the  $\text{BaTiO}_3$  particles was 0.013wt% in the colloidal mixture.

The detailed procedure for cell preparation is given elsewhere [6,7,17,18]. The cell thickness  $\approx 2 \mu\text{m}$  was maintained for *LF4*/ $\text{LiNbO}_3$  and *LNSM6*/ $\text{BaTiO}_3$  nanocolloids experiments by using ball spacers. *LF4*/ $\text{LiNbO}_3$  nanocolloids were studied in the planar cell prepared by rubbing the polymer films 50 times in one direction. While, *LNSM6*/ $\text{BaTiO}_3$  nanocolloids were studied in the 20 times and 50 times rubbed planar cell.

In order to study the effect of varying the polymer layer thickness on the various parameters of FLCs three solutions with 5, 15 and 25% wt% Nylon 6 in 2,2',2''-trichloroethanol were prepared. The solutions with different polymer concentrations were spin coated at 3500 rpm for three minutes on the ITO coated glass plates to obtain films of different thickness. Thicknesses 35 nm, 78 nm and 142 nm were measured for the films deposited from the

solutions. Varying the polymer layer studies were done in 50 times rubbed planar cells. The cell thickness for varying the polymer layer studies was fixed  $\approx 3.5 \mu m$ .

We carried out all characterizations in the heating cycle. A setup including a He-Ne laser at a wavelength of  $\lambda = 632.8 \text{ nm}$ , a rotating table, a Linkam LTS 350 hot stage attached controlled with a Linkam CI 94 temperature controller (with an accuracy  $\pm 0.1^\circ \text{C}$ ), a function generator HP 33120A, and a digital oscilloscope HP Infinium were used for measuring the electrooptic parameters. The frequency and the strength of the bipolar rectangular electric field used for all of the electrooptic measurements were  $3 \text{ Hz}$  and  $10 \text{ V}/\mu m$ , while,  $15 \text{ V}/\mu m$  was used for polarization measurements. The accuracy for the switching time was  $\pm 1 \mu s$ , for tilt angle  $\pm 1^\circ$  and for the  $P_s \pm 1 \text{ nC}/\text{cm}^2$ . A reverse current technique with a triangular wave electric field was used for the  $P_s$  measurements [19]. Dielectric measurements were carried out using an impedance analyzer 4192A (frequency range:  $100 \text{ Hz}$  to  $1 \text{ MHz}$ , probing voltage:  $100 \text{ mV}$ ).

## Results and discussion

### Case 1- LF4 /LiNbO<sub>3</sub> nanocolloids

The thermo-optical texture measurements of the LF4/LiNbO<sub>3</sub> nanocolloids were carried out in order to check the alignment quality. Well aligned optical textures (not shown here) were observed for 0.01wt% and 0.1 wt% LF4/LiNbO<sub>3</sub> nanocolloids reflecting the dopant was homogeneously dispersed in the FLC matrix. No noticeable change in the transition temperature after the addition of nanoparticles could be registered, which also suggested the homogeneity of the nanocolloids.

The temperature dependent electro-optic parameters for the undoped LF4 and LF4/LiNbO<sub>3</sub> nanocolloids are presented in figure 1 (a, b & c). No significant change was observed in the tilt angle for nanocolloids at either concentration (0.01 and 0.10 wt. %) (Fig. 1 a) compared to the undoped LF4 which indicates that the dopant LiNbO<sub>3</sub> did not perturb the smectic layers of LF4. On the other hand, a significant change has been seen in the switching time ( $\tau$ ) with increasing dopant concentration (0.01 to 0.10 wt%) as depicted in the figure 1 b. About 45% reduction has been observed for the higher dopant concentration compared to the undoped LF4. The  $P_s$  also follows the same trend as  $\tau$ . A decrease in  $P_s$  with increased dopant concentration is evident from the figure 1 c. However, the reduction in  $P_s$  is not as prominent as for  $\tau$ .

Considering these results it is reasonable to say that doping of LiNbO<sub>3</sub> strongly influence the electro-optical parameters particularly  $\tau$  and to some extent  $P_s$ . A probable reason could be an increase in the localized electric field in nanocolloids. The localized electric field  $\vec{E}_{loc}$  for undoped FLC and FLC/LiNbO<sub>3</sub> nanocolloids can be estimated by using the relation  $\gamma_\varphi = \tau P_s \vec{E}_{loc}$  (where  $\gamma_\varphi$  is the rotational viscosity). The calculated magnitude of  $\vec{E}_{loc}$  for the undoped LF4 and 0.01 and 0.1wt.% LiNbO<sub>3</sub> doped nanocolloids are 30.0, 36.4 and 61.0  $\text{V}/\mu m$  respectively. Such an increase in the  $\vec{E}_{loc}$  with LiNbO<sub>3</sub> doping can be understood via ion capturing on the surface of LiNbO<sub>3</sub> nanoparticles which significantly hinder the migration of the ions to the walls of the cells. The complete model for such a phenomenon has been earlier reported for FLC/LiNbO<sub>3</sub> nanocolloids [7]. Trapping of ions and an increase in the localized electric field allows for a faster the switching time, while, the decrease in the  $P_s$  is attributed to the anti-parallel coupling among harvested nano particles and the LF4

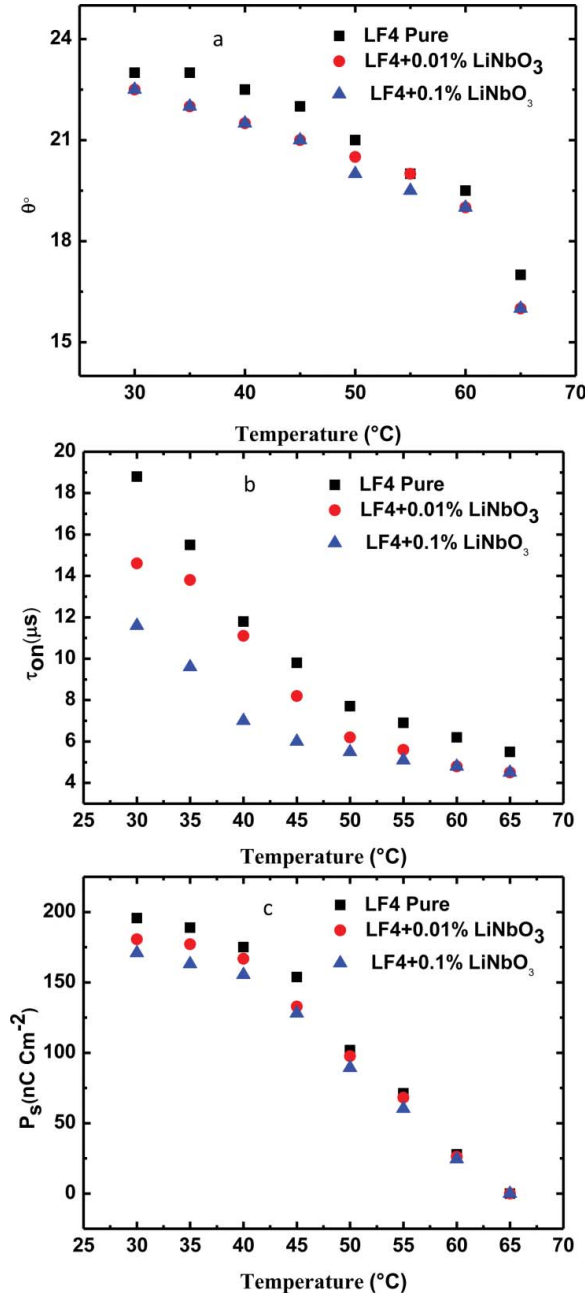


**Figure 1.** Temperature dependence of (a) tilt angle, (b) switching time ( $\tau$ ) and (c) spontaneous polarization ( $P_s$ ) for non-doped LF4 and LiNbO<sub>3</sub>/LF4 nanocolloids.

molecules. Another reason is that the capturing of ions can also screen the net dipole moment and hence reduces the  $P_s$  [7]. Such effects are well established for many FLC nanocolloids and have been explained by considering a different transport mechanism at the interface [7,17,18]. In general what has been presented in [7] tilt angle (independent), switching time (decreased by increasing amount of dopant), spontaneous polarization

(slightly decreased by increasing the amount of dopant) are in good agreement with the presented results. This means the tendency of changing the electrooptic parameters does not depend on the absolute value of  $P_s$  for the given FLC nanocolloid resulting in a partially anti-parallel dipole compensation.

The frequency dependent complex permittivity ( $\epsilon'$  and  $\epsilon''$ ) for the undoped *LF4* and 0.01 and 0.1wt% nanocolloids is shown in figure 2 (a, b). A significant decrease of about 50% in the dielectric constant for *LF4*/LiNbO<sub>3</sub> dispersions compared to undoped *LF4* can be seen. For 0.01% doping concentration the  $\epsilon'$  is gradually different compared to 0.01% presented in [7]. Presumably the ions are more strongly captured due to higher values of  $P_s$  in the *LF4* nanocolloids compared to those in [7]. Similarly, the strong reduction in the absorption maxima has also been seen with doping concentrations (0.01 and 0.1wt %), viz.  $\epsilon''$  maxima reduced from 6 to  $\approx 2$  compared to undoped *LF4*. For FLC/LiNbO<sub>3</sub> 0.01% compared to [7] this is slightly different due to higher ion capturing because of larger  $P_s$ . Well defined absorption peaks seen in the *kHz* range for the undoped *LF4* and nanocolloids are due to the collective contribution of Goldstone mode process (Fig. 2 b).

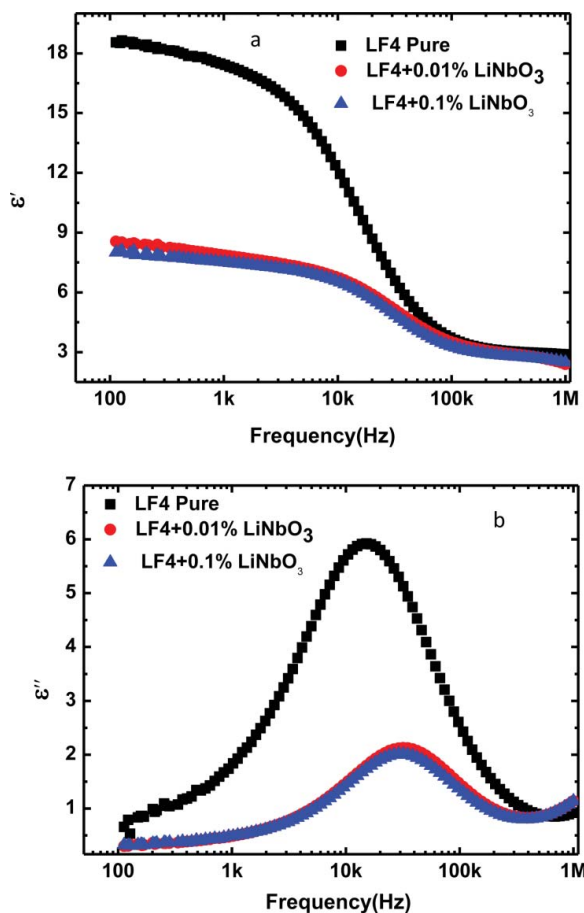


**Figure 2.** Frequency dependence of (a) dielectric permittivity, (b) absorption strength for non-doped *LF4* and LiNbO<sub>3</sub>/*LF4* nanocolloids at temperature 30°C.

### Case 2- BaTiO<sub>3</sub> / LNSM6 nanocolloids

As introduced above, BaTiO<sub>3</sub> with an average diameter 26  $\mu\text{m}$  were studied by performing electrooptic and dielectric experiments using the FLC mixture LNSM6 [6]. For the current experiment we wanted to study the influence of the number of rubbing cycles done by hand on the polymer layer Nylon 6 with a Nylon cloth. The motivation for doing so was to answer the question is there in general an influence of the rubbing cycles above a certain number on the electrooptic and dielectric parameters and furthermore, does there exist a special effect due to ferroelectric nanoparticles. It is well known, 50 times repetition by hand is generally considered as the gold standard. Here the effect of commercial rubbing by using a machine will not be considered.

The temperature dependences of the  $P_s$  for 0.013 wt % LNSM6/BaTiO<sub>3</sub> with 26 nm (average) diameter nanoparticles measured in different but analogously prepared cells manufactured with 20 times and 50 times rubbing by hand in parallel manner are presented in figure 3.  $P_s$  for 50 times rubbing agrees with the data presented in Ref. 6 while those for 20 times have reduced  $P_s$  values compared to 50 times rubbing. The observation, that both  $P_s$  and  $\tau$ , not shown here, are increased by a larger number of rubbing cycles could be explained on the basis of both weaker alignment during 20 times rubbing and the capturing of ions in the samples via less rubbing. Change of anchoring energy  $W$  plays a role too, discussed under case 3.

Capturing of ions may enhance  $\vec{E}_{loc}$  and hence reduce  $P_s$  and  $\tau$ , more for 20 times rubbed than for 50 times rubbed. Less number of ions in the 20 times rubbed cell confirm that less rubbed surfaces also act as a charge trap channel that can screen the charge transport mechanism at the surface and decrease the influence of ionic contributions. This argument is further supported with dielectric and conductivity measurements.

Frequency dependent dielectric data for 0.013wt % LNSM6/BaTiO<sub>3</sub> nanocolloids measured in different cell with 20 times and 50 times rubbing are shown in figure 4 a, b. The dielectric constant is found to be less for the 20 times rubbed cell than the 50 times rubbed cell. Similarly, the absorption factor goes down for the less rubbed cell (20 times). The observed effect is caused by less alignment in the 20 time rubbed cell and by the same time

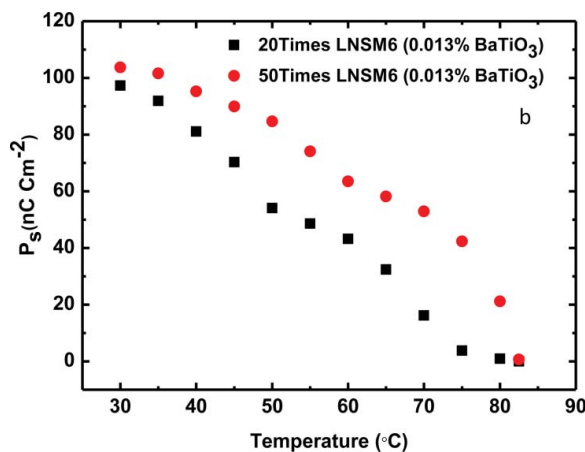


**Figure 3.** Temperature dependence of spontaneous polarization ( $P_s$ ) for 20 times and 50 times rubbed cells.

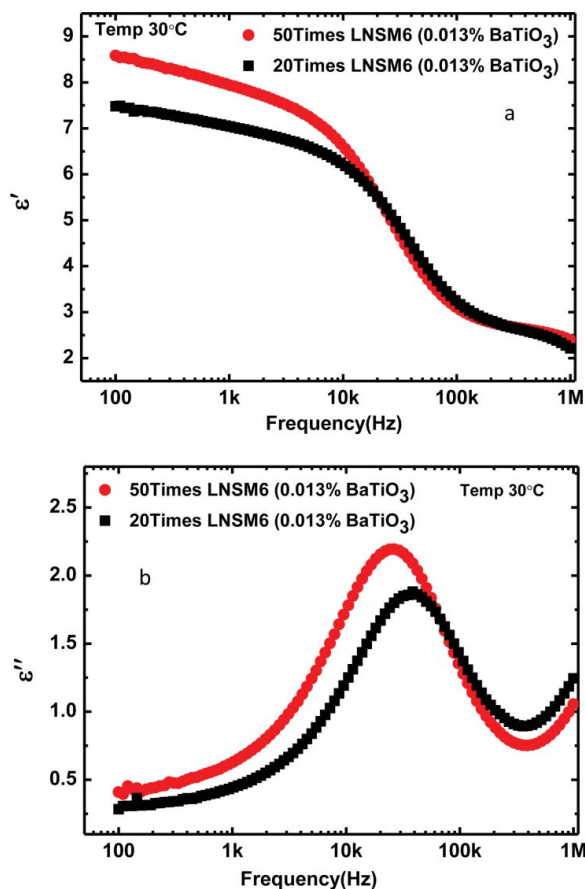


**Figure 4.** Frequency dependence of (a) dielectric permittivity, (b) absorption strength for 20 times and 50 times rubbed cells at temperature 30°C.

the limited availability of surface charges for transport phenomena at the interface due to the reduced amount of free ions. Furthermore, the argument is also supported by the conductivity measurement of  $\sigma_{ac}$ , where  $\sigma_{ac} = \epsilon_0 \epsilon'' \omega$  with  $\epsilon_0$  static dielectric constant,  $\epsilon''$  dielectric absorption,  $\omega$  absorption frequency. We found less  $\sigma_{ac}$  for the 20 times rubbed cell  $\approx 5.8 \times 10^{-9} \text{ Sm}^{-1}$  as compared to the 50 times rubbed cell  $\sigma_{ac} \approx 6.9 \times 10^{-9} \text{ Sm}^{-1}$ .

### Case 3- Polymer layer thickness dependent studies

Based on our own experience the optimum thickness of the Nylon 6 polymer is between 60 and 80 nm. In the searching for the influence of polymer layer thickness on the electrooptic and dielectric parameters we used cells of the same FLC thickness ( $\approx 3.5 \mu\text{m}$ ), same rubbing times (50 times), same polymeric material Nylon 6, but changed the Nylon 6 polymer layer thickness. The ferroelectric mixture used for these studies was LF4. The temperature dependence of electro-optic parameters as a function of the polymer layer thickness dependent experiments (35 nm, 78 nm and 142 nm) are presented in the figure 5 a, b, c. The tilt angle is stable within the error bar as shown in fig. 5c. It was observed that the switching time gets faster as the thickness of the

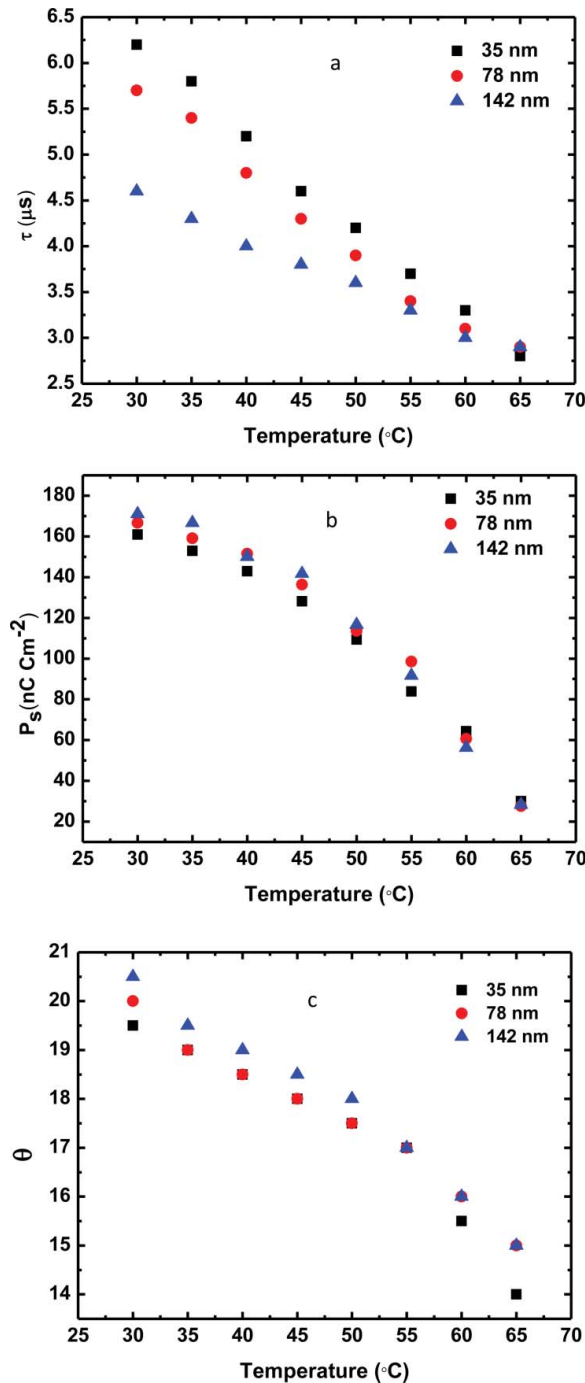


**Figure 5.** Temperature dependence of (a) switching time ( $\tau$ ), (b) spontaneous polarization ( $P_s$ ) and (c) tilt angle for 35 nm, 78 nm and 142 nm polymer layer thickness samples.

polymer layer is increased while between 35 nm and 78 nm there is only a small difference within the error bar (fig. 5a). The  $P_s$  shows a slightly adverse effect (fig. 5c), almost outside the error bar.

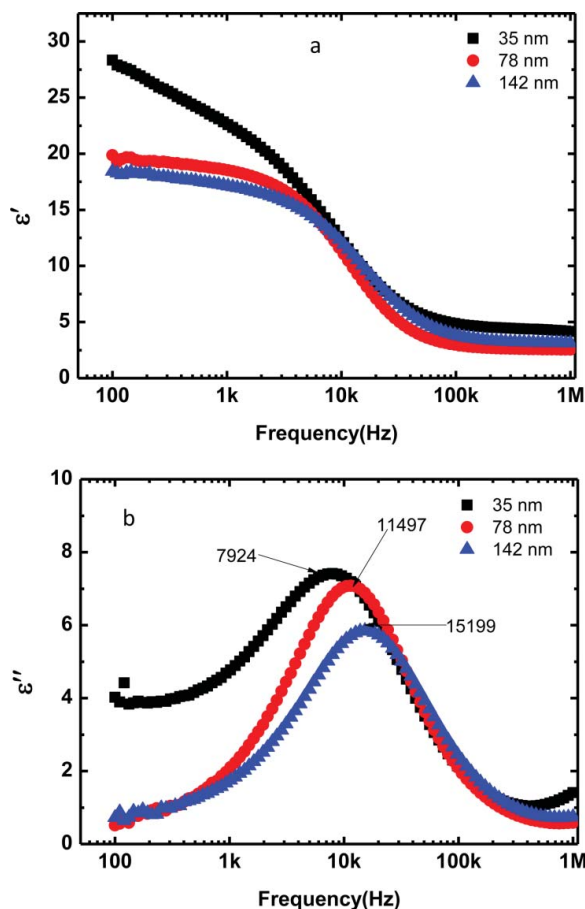


**Figure 6.** Frequency dependence of (a) dielectric permittivity, (b) absorption strength for 35 nm, 78 nm and 142 nm polymer layer thickness samples at temperature 30°C.

The effect of the thickness of the polymeric layer is similar to the repetitions of rubbing cycles (*Case 2*) directly related to the change of the surface, with other words to the change of the electrical potential at the surface. Different layer thicknesses lead to a different surface potential. Rubbing influences the surface in forming grooves and uploading the surface due to an electrical potential leading to alignment of next layers of liquid crystals molecules.

Basically the anchoring energy  $W$ , usually between  $10^{-4}$  and  $10^{-5}$   $J/m^2$  [20], is following Ref. 14 inversely proportional to switching time  $\tau = 4 \gamma_{\phi} d/W \pi^2$ , where  $\gamma_{\phi}$  is the rotational viscosity and  $d$  the cell thickness. As  $d$  is constant, one can presume the anchoring energy increases with an increase of the rubbed polymer layer thickness leading to a further reduction of switching time. As a consequence for practical applications one should fix the polymer layer thickness more or less as constant near the optimum 60-80 nm for comparable experiments.

The dielectric spectroscopy results for the samples having 35 nm, 78 nm and 142 nm polymer layer thickness are presented in fig. 6 a.b. The dielectric constant decreases with an increase of the polymer layer thickness as evident from figure 6 a. Similarly, the absorption factor  $\epsilon''$  goes down with an increase in thickness, fig. 6b.

Another aspect is the increase of the polymer layer thickness suppresses the conductivity leading to decrease of dielectric parameters. AC conductivity has been calculated for three samples with 35 nm, 78 nm and 142 nm polymer layer thickness leading to  $7.8 \times 10^{-9}$ ,  $4.0 \times 10^{-9}$  and  $3.2 \times 10^{-9} \text{ Sm}^{-1}$  respectively.

## Conclusion

We used a very high- $P_s$  FLC (LF4) for the investigation of the LF4/LiNbO<sub>3</sub> mixture. In agreement with former investigations using a FLC with a lower  $P_s$  we could demonstrate that there is always partially antiparallel compensation of the dipoles of the harvested solid state nanoparticle with the dipoles of the FLC structure scaled on the decrease of  $P_s$ . The switching time has been reduced while the tilt angle is unchanged. The observed behavior may be attributed to charge capture at the surface of the harvested LiNbO<sub>3</sub> nanoparticles, which increases the localized electric field  $\vec{E}_{loc}$ .

Cell parameters have pronounced influence on the medium FLC/nanocolloid, studied on the LNSM6/BaTiO<sub>3</sub> system, where LNSM6 showed an average  $P_s$ . Different amount of rubbing procedures influences electrooptic and dielectric parameters to a strong extent: an increase of rubbing cycles leads to a slight increase of both switching times and  $P_s$ .

Rubbing forms grooves into the polymer layer, but also upload the polymer layer with electrical charges leading to an increase of the anchoring energy. The anchoring forces are strongly influenced by the thickness of the polymer layer lowering the switching time by increasing the polymer layer thickness. This has been demonstrated for the high- $P_s$  FLC LF4.

## Acknowledgment

We thank Dr. V. Lapanik for valuable comments.

## References

1. S. T. Lagerwall *Ferroelectric and Antiferroelectric Liquid Crystals*, Wiley-VCH, Weinheim, 1999.
2. I. Musevic, R. Blinc, B. Zeks *The Physics of Ferroelectric and Antiferroelectric Liquid Crystals*, World Scientific, Singapore, New Jersey, London, Hong Kong, 2000.
3. V. Lapanik, V. Bezborodov, G. Sasnousky, W. Haase *Liquid Crystals* **40**, 1391 (2013).
4. V. Lapanik et al. *Liquid Crystals*, in print.
5. Y.A. Garbovsky and A.V. Glushchenko *Liquid Crystalline Colloids of Nanoparticles: Preparation, Properties, and Application*, *Solid State Physics* **62**, 1–74 (2011).
6. A. Rudzki, D. R. Evans, G. Cook and W. Haase *Appl. Opt.*, **52**, 22 (2013).
7. R. K. Shukla, C. M. Liebig, D.R. Evans, and W. Haase *RSC Adv.*, **4**, 18529 (2014).
8. S. A. Basun, G. Cook, V. Y. Reshetnyak, A. V. Glushchenko and D. R. Evans *Phys. Rev. B: Condens. Matter Mater. Phys.*, **84**, 024105 (2011).
9. G. Cook, J. L. Barnes, S. A. Basun, D. R. Evans, R. F. Ziolo, A. Ponce, V. Y. Reshetnyak, A. V. Glushchenko and P. P. Banerjee *J. Appl. Phys.*, **108**, 064309 (2010).
10. A. Mikulko, P. Arora, A. Glushchenko, A. Lapanik, W. Haase *Europhys. Lett.* **87**, 27009 (2009).
11. P. Kumar and A. Sinha *Phase Transitions* **88**, 60510 (2015).
12. J. Prakash, A. Chandran, A. Malik and A.M. Biradar *Liquid Crystals* **42**, 1748 (2015).
13. D. Shenoy, A. Lavarello, J. Naciri and R. Shashidhar *Liquid Crystals* **28**, 841 (2001).
14. X. Nie, R. Lu, H. Xianyu, T.X. Wu and S.-T. Wu *J. Appl. Phys.* **101**, 103110 (2007).

15. H. Atkuri, G. Cook, D.R. Evans, C.-I.Cheon, A. Gluschen, V. Reshetnyak, Yu Reznikov, J. West and K. Zhang *Journal of Optics A: Pure and Appl. Optics* 024006 (2009).
16. D.R. Evans, S.A. Basun, G. Cook, I.P. Pinkevych, and V. Yu Reshetnyak *Phys.Rev. B* **84**, 174111 (2011).
17. F. V. Podgornov, A. V. Ryzhkova and W. Haase *Appl. Phys. Lett.*, **97**, 212903 (2010).
18. R. K. Shukla, K. K. Raina and W. Haase *Liq. Cryst.*, **41**, 1726 (2014).
19. K. Miyasato, S. Abe, H. Takezoe, A. Fukuda, E. Kuze *Jpn. J. Appl. Phys.*, **22**, 66 (1983).
20. C. Gear, K. Diest, V. Liberman and M. Rothschild *Optics Express* **23**, 807 (2015).

# REPORT DOCUMENTATION PAGE

*Form Approved*  
OMB No. 0704-0188

The public reporting burden for this collection of information is estimated to average 1 hour per response, including the time for reviewing instructions, searching existing data sources, gathering and maintaining the data needed, and completing and reviewing the collection of information. Send comments regarding this burden estimate or any other aspect of this collection of information, including suggestions for reducing this burden, to Department of Defense, Washington Headquarters Services, Directorate for Information Operations and Reports (0704-0188), 1215 Jefferson Davis Highway, Suite 1204, Arlington, VA 22202-4302. Respondents should be aware that notwithstanding any other provision of law, no person shall be subject to any penalty for failing to comply with a collection of information if it does not display a currently valid OMB control number. **PLEASE DO NOT RETURN YOUR FORM TO THE ABOVE ADDRESS.**

<b>1. REPORT DATE (DD-MM-YY)</b> 17 September 2016		<b>2. REPORT TYPE</b> Interim		<b>3. DATES COVERED (From - To)</b> 26 October 2015 – 17 August 2016	
<b>4. TITLE AND SUBTITLE</b> FERROELECTRIC BaTiO <sub>3</sub> AND LiNbO <sub>3</sub> NANOPARTICLES DISPERSED IN FERROELECTRIC LIQUID CRYSTAL MIXTURES: ELECTROOPTIC AND DIELECTRIC (POSTPRINT)				<b>5a. CONTRACT NUMBER</b> FA8650-16-D-5402-0001	
				<b>5b. GRANT NUMBER</b>	
				<b>5c. PROGRAM ELEMENT NUMBER</b>	
<b>6. AUTHOR(S)</b> 1) R.K. Shukla and W. Haase – Technische Universität Darmstadt 2) D.R. Evans – AFRL/RX				<b>5d. PROJECT NUMBER</b>	
				<b>5e. TASK NUMBER 0001</b>	
				<b>5f. WORK UNIT NUMBER</b> X14Z	
<b>7. PERFORMING ORGANIZATION NAME(S) AND ADDRESS(ES)</b> 1) Technische Universität Darmstadt Hochschulstr. 1 · 64289 Darmstadt Germany 2) AFRL/RX Wright Patterson AFB, OH 45433				<b>8. PERFORMING ORGANIZATION REPORT NUMBER</b>	
<b>9. SPONSORING/MONITORING AGENCY NAME(S) AND ADDRESS(ES)</b> Air Force Research Laboratory Materials and Manufacturing Directorate Wright-Patterson Air Force Base, OH 45433-7750 Air Force Materiel Command United States Air Force				<b>10. SPONSORING/MONITORING AGENCY ACRONYM(S)</b> AFRL/RXAP	
				<b>11. SPONSORING/MONITORING AGENCY REPORT NUMBER(S)</b> AFRL-RX-WP-JA-2017-0210	
<b>12. DISTRIBUTION/AVAILABILITY STATEMENT</b> Distribution Statement A. Approved for public release: distribution unlimited.					
<b>13. SUPPLEMENTARY NOTES</b> PA Case Number: 88ABW-2016-4583; Clearance Date: 17 Sep 2016. This document contains color. Journal article published in Ferroelectrics. © 2016 Taylor & Francis Group, LLC. The U.S. Government is joint author of the work and has the right to use, modify, reproduce, release, perform, display, or disclose the work. The final publication is available at <a href="http://dx.doi.org/10.1080/00150193.2016.1215206">http://dx.doi.org/10.1080/00150193.2016.1215206</a>					
<b>14. ABSTRACT (Maximum 200 words)</b> Harvested ferroelectric nanoparticles of BaTiO <sub>3</sub> and LiNbO <sub>3</sub> were dispersed in Ferroelectric Liquid Crystals (FLCs) with very high spontaneous polarization (Ps). The electrooptic and dielectric parameters were documented. The dipoles of ferroelectric nanoparticles and those of FLCs are partially cancelled in an antiparallel manner. The role of cell parameters like thickness of the Nylon 6 polymer layer and the change in preparation of the polymer layer due to different mechanical rubbing cycles has been described for one high-Ps FLC and for high-Ps FLC/BaTiO <sub>3</sub> nanocolloids. Cell properties depend strongly on anchoring forces which might interact with dipoles both from ferroelectric nanoparticles and high-Ps FLCs.					
<b>15. SUBJECT TERMS</b> Ferroelectric liquid crystals, solid state ferroelectrics, FLC-nanocomposites, surface phenomena					
<b>16. SECURITY CLASSIFICATION OF:</b>			<b>17. LIMITATION OF ABSTRACT:</b> SAR	<b>18. NUMBER OF PAGES</b> 14	<b>19a. NAME OF RESPONSIBLE PERSON (Monitor)</b> Shekhar Guha <b>19b. TELEPHONE NUMBER (Include Area Code)</b> (937) 255-0119
<b>a. REPORT</b> Unclassified	<b>b. ABSTRACT</b> Unclassified	<b>c. THIS PAGE</b> Unclassified			